Impurity Transport Experiments at the HSX Stellarator

Presenter: J. Fernando Castillo

B. Geiger, A. Bader, S.T.A. Kumar, K.M. Likin, D.T. Anderson

HSX Plasma Laboratory, Univ. of Wisconsin-Madison, USA

63rd Annual Meeting of the APS Division of Plasma Physics

November 8-12, 2021. Pittsburgh, PA

 This work is supported by US DOE Grant DE-FG02-93ER5422

Motivation and goals of this study

Motivation to study impurity transport:

- Impurities dilute fuel and radiate away energy from the plasma
    - Too much He ‘ash’ in core
    - Wall-sourced impurities accumulate
- Predict and control impurity accumulation
    - Impurity transport is a serious constraint and needs to be better understood in 3-D fusion devices

HSX Stellarator

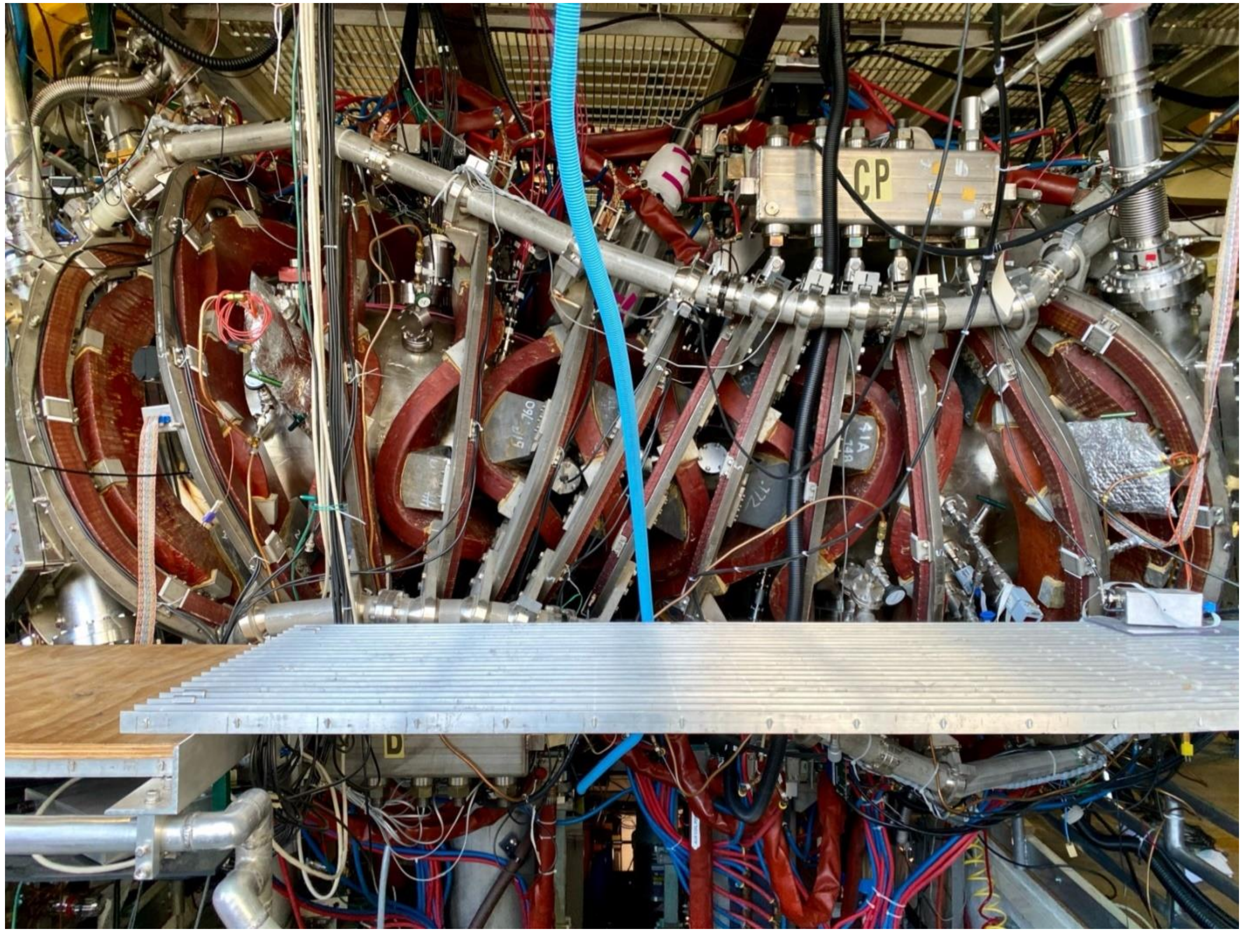

Goals of this study:

- Quantify impurity transport properties of the HSX stellarator
- Compare these results to neoclassical calculations to determine whether transport is anomalous

Talk outline

- **Introduction**
- **Experimental Set-up and Data Collection**
- **Computational Modeling and Analysis**
- **Experimental Findings**
- **Summarize Key Results**

Neoclassical theory predicts impurity accumulation

Law of Particle Conservation

$$\frac{\partial n_{I,z}(r)}{\partial t} = -\nabla \cdot \underbrace{\Gamma_{I,z}(r)}_{\left(-D\nabla n_{I,z} + v n_{I,z}\right)} + Q_{I,z}(r)$$

Positive impurity flux density $\Gamma_{I,z}$ correlates to an outward flux

- $Q_{I,z}$ – sources and sinks due to ionization, recombination and charge exchange
- Positive v indicates the convection direction is outward whereas a negative $\boldsymbol{v}$ is inwards

Neoclassical Particle Flux Density

$$\Gamma_I^{nc} = -D_{11} \cdot \nabla n_I + \underbrace{\left(D_{11}\frac{qE_r}{T_I} - D_{12}\frac{\nabla T_I}{T_I}\right)}_{v_{nc}} \cdot n_I$$

Velocity is dependent on the electric field

- **Electron root confinement** **–** Stronger flux drift of electrons to ions leads to positive, outward-directed E_r
- **Ion root confinement –** Inward-directed E_r may cause impurity ion accumulation which should be avoided

HSX is optimized for improved neoclassical transport.

What happens with impurity transport?

Introduction to the HSX Stellarator

Helically **S**ymmetric e**X**periment

- Optimized Stellarator – **Q**uasi-**H**elical **S**ymmetry
- 4 field periods, 12 modular coils per period
- 48 auxiliary coils for configuration flexibility

'Typical' plasma discharge

- QHS, 1 Tesla, 44 kW injected power
- Line-averaged electron density of 3×10^{18} m^{-3} (reproducibility)
- Absorbed ECH power is ≈ 11.3 kW, deposited on-axis

Electron Temperature

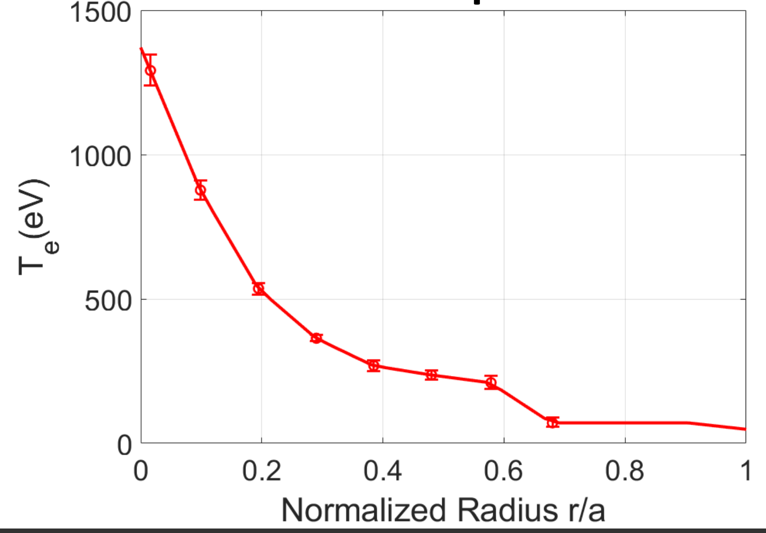

Electron Density

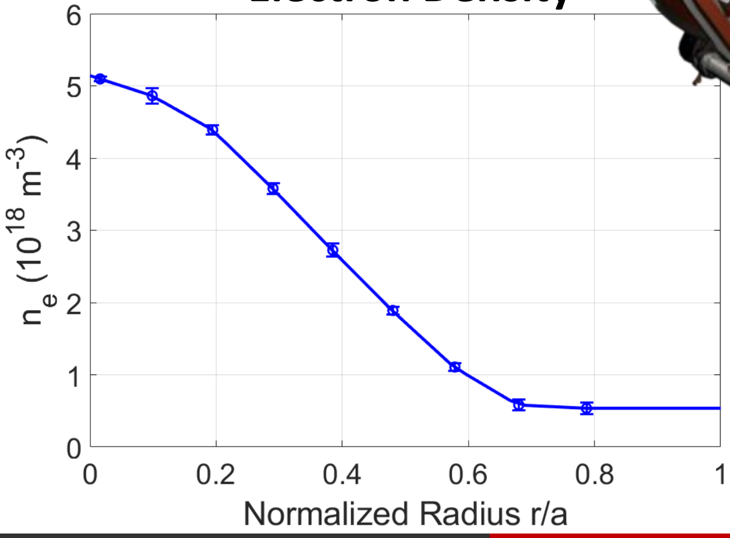

HSX Cutaway Rendering

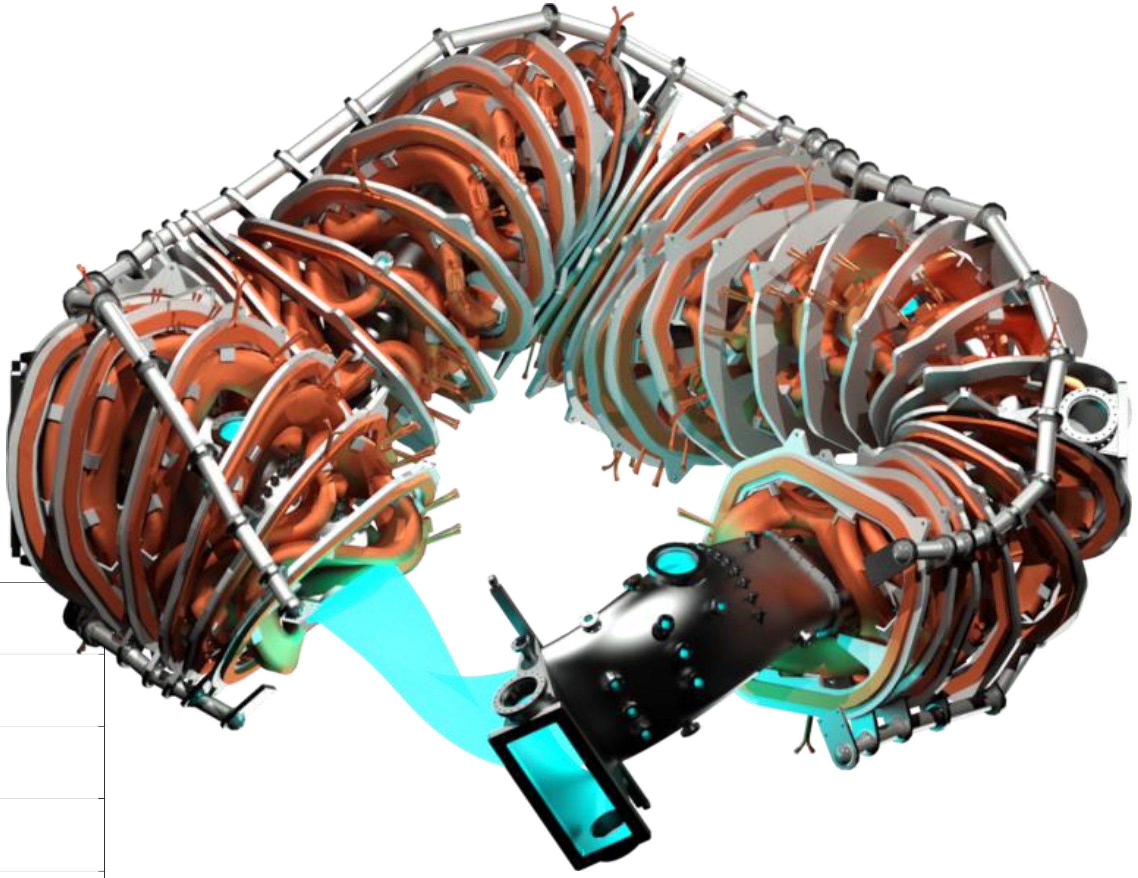

Impurity injection by laser blow-off (LBO)

LBO technique is used at C-Mod, JET, TJ-II, W7-AS, W7-X and more

- A laser illuminates a thin film of tracer material (aluminum) on a target
- Resulting neutrals ballistically enter plasma and emit radiation
- Quantity of neutrals is controllable
- Photodiode detectors measure impurity radiation

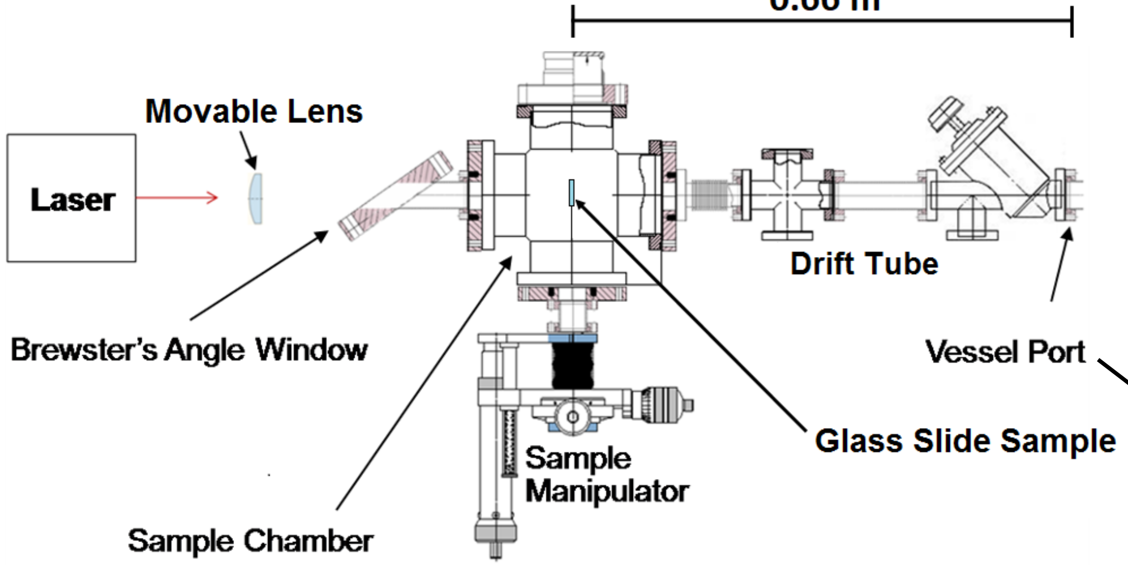

Schematic of HSX LBO System

Photodiode Arrays

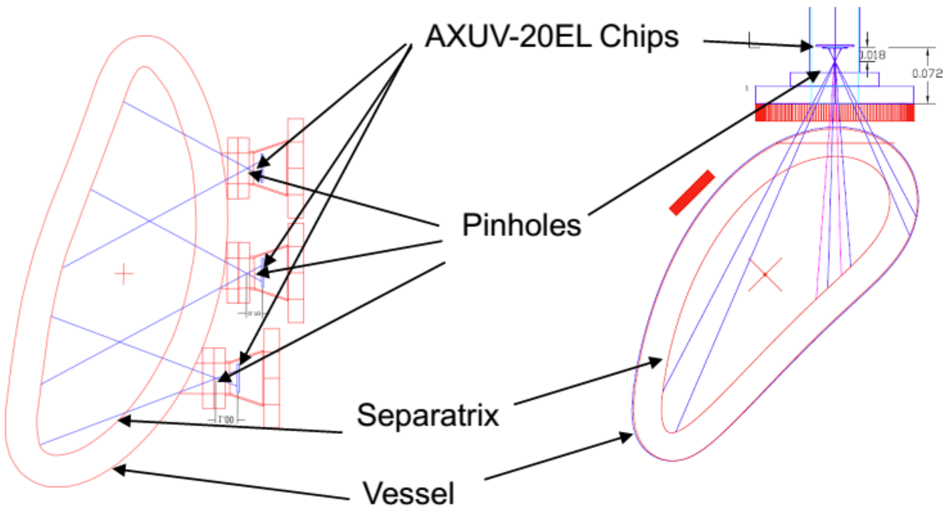

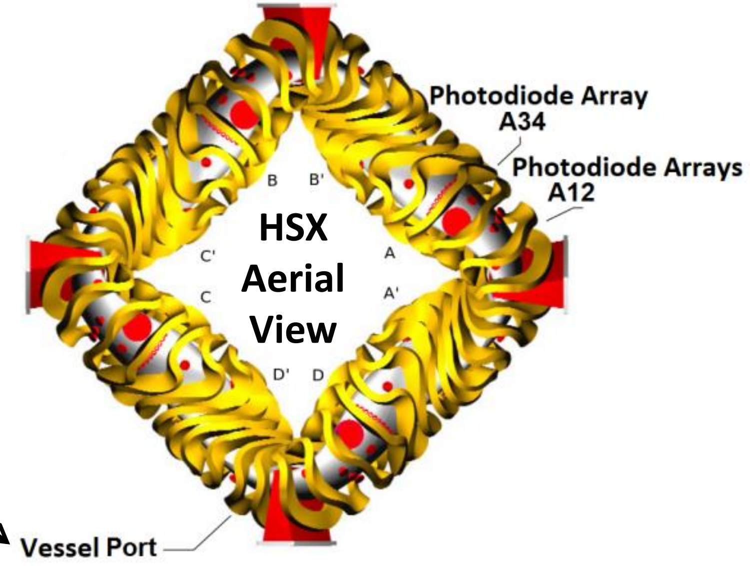

Good signal-to-noise ratio without strong density perturbation

LBO experimental results – 'Typical' QHS plasma discharge

- Aluminum neutrals penetrate into plasma before ionizing
- Photodiode arrays covers the spectral range of 0.4 nm to 1100 nm
- Signals provide line-integrated measurements of local emissivity
- Channel 11 of array A12M is closest to center of core

Photodiode Array lines-of-sight

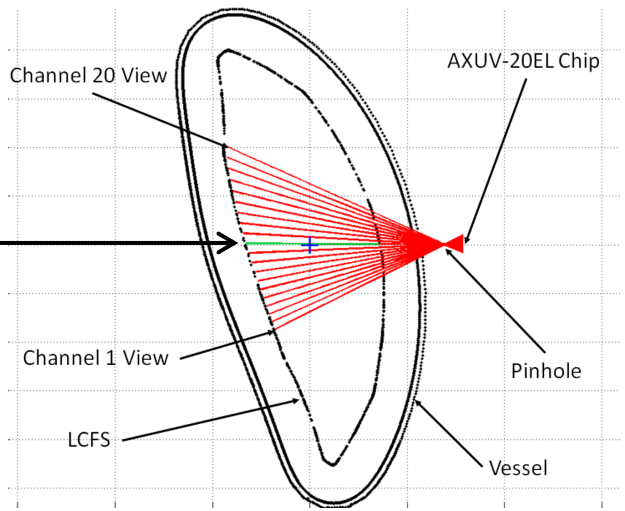

Line-averaged Electron Density

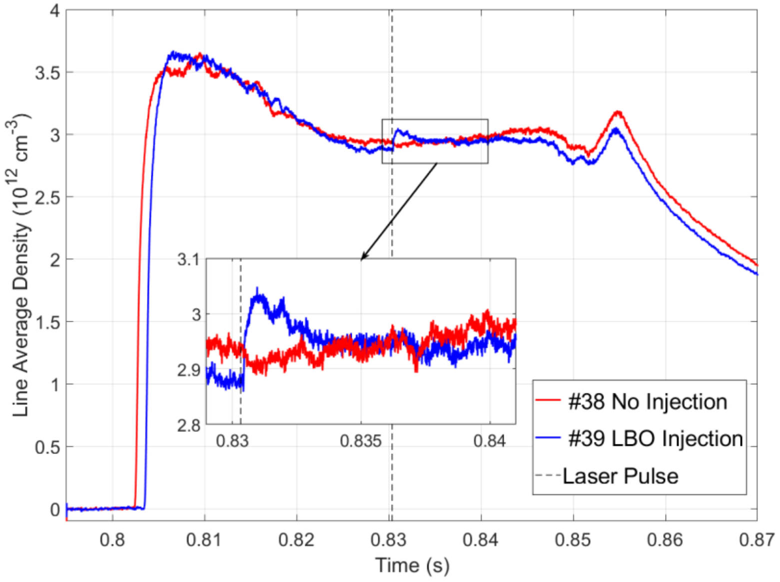

A12M 'Core' Channel 11

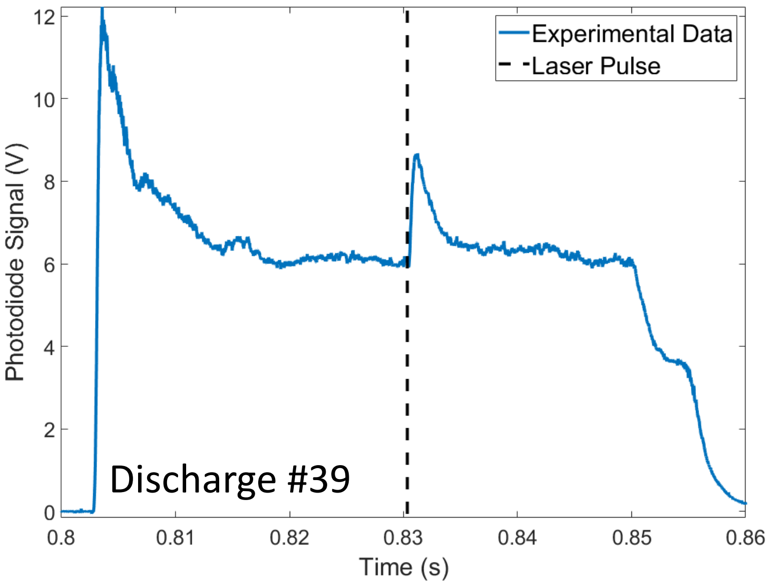

Experimental A12M Array Signals

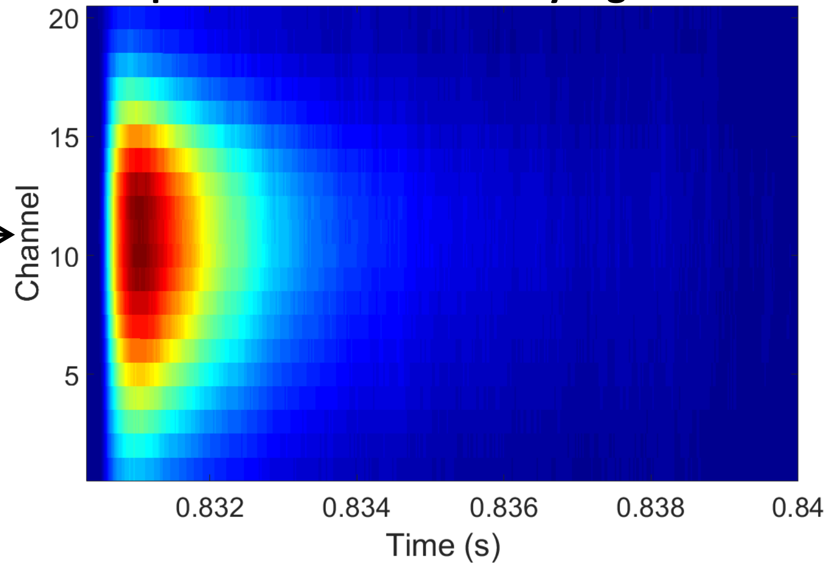

Castillo, J.F. et al., JINST 040P 0621 (2021).

STRAHL code is used for computational analysis

STRAHL is a 1D transport code that solves the radial continuity equation of all impurity charge states

$$\frac{\partial n_{I,z}}{\partial t} = \frac{1}{r}\frac{\partial}{\partial r} r \left(D \frac{\partial n_{I,z}}{\partial r} - v n_{I,z} \right) + Q_{I,z}$$

Dux, R., STRAHL User Manual, (2006).

Inputs

- Cylindrical plasma geometry
- ADAS (Atomic Data and Analysis Structure) database
- Experimental radial profiles of T_e, n_e, T_I and n_H
- Impurity neutral source rate function, scrape-off layer loss time τ_{sol}
- Impurity transport coefficients – user provided

$$D = 3.0 \ \left(\mathrm{m}^2/\mathrm{s}\right), v = 0 \ \left(\mathrm{m}/\mathrm{s}\right)$$

Outputs

- Total impurity emissivity $\boldsymbol{\varepsilon_{tot}}$ $\left(\mathbf{W}/\mathbf{m^3}\right)$ after LBO discharge
- Sum of all aluminum charge states
- Strong intensity occurs 1 ms after LBO discharge

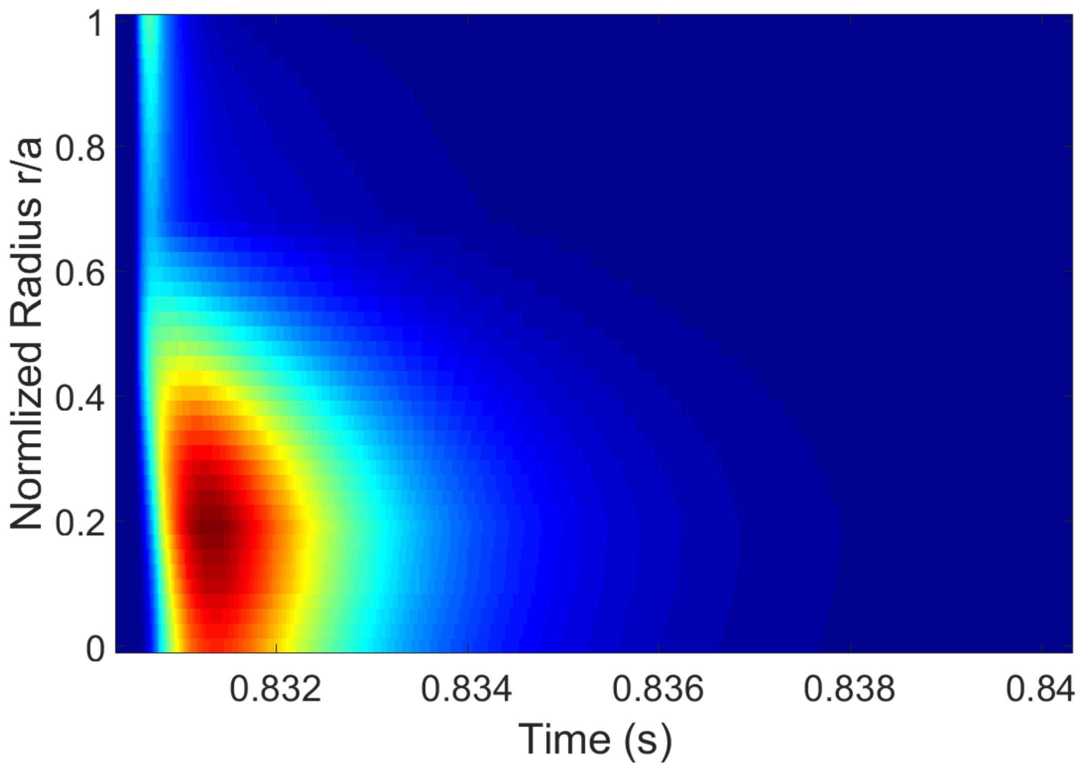

Synthetic diagnostic output is compared to experimental signals

Brightness – Line-integrated plasma emissivity

$$B_x = \iint \varepsilon_{tot}(x,\lambda)\mathcal{R}_\lambda \, d\lambda \, dl$$

$\boldsymbol{\varepsilon_{tot}}$ modeled by STRAHL, diode responsivity $\boldsymbol{\mathcal{R}_\lambda}$ from data sheet

1. Discretize detector sightline vectors
   - Each detector line-of-sight has a lab coordinate entry and exit point at the LCFS
2. Convert lab coordinate vector values x to ρ using VMEC equilibrium
3. $\varepsilon_{\mathrm{tot}}$ at a given radius and time is interpolated from STRAHL result
4. Calculate $\iint \varepsilon_{tot}(x,\lambda)\mathcal{R}_\lambda \, d\lambda \, dl$
   - All individual Al wavelengths between 0.4 and 1100 nm considered

Simulated signals are obtained using a synthetic diagnostic

Experimental Photodiode Signals

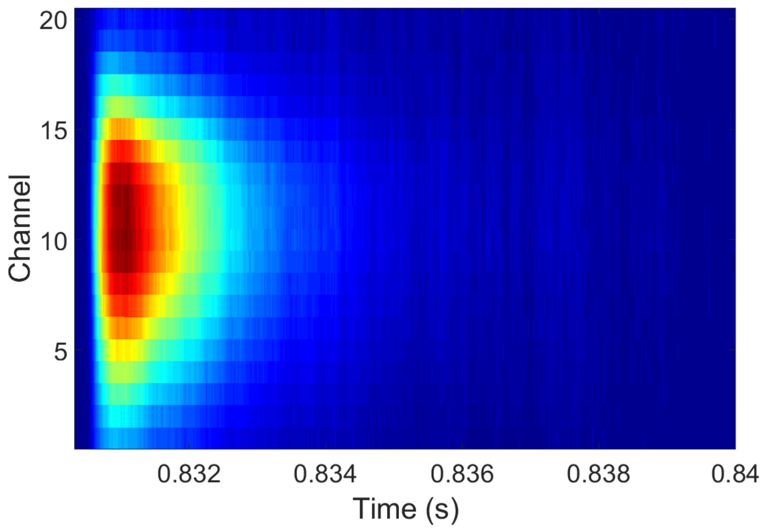

Simulated Photodiode Signals

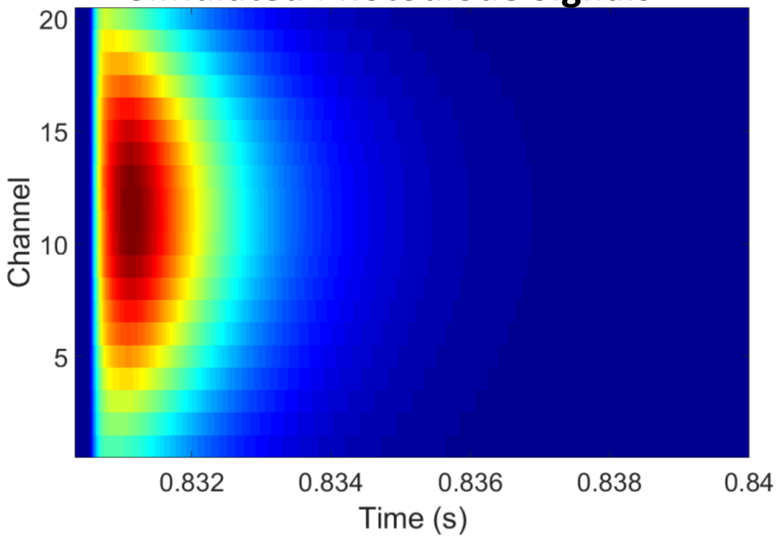

Optimization algorithm provides best fit for data

Objective – Generate D values consistent with data

- Optimization algorithm, with D acting as a free parameter, is used in conjunction with STRAHL-modeled synthetic diagnostic
- Minimize difference between modeled simulated signals and experimental measurements

Least-squares Data Fitting Method

$$\min_x \sum_j \sum_i w_j \left[f_{1,1}(x)^2 + f_{1,2}(x)^2 + \cdots f_{j,i}(x)^2 \right]$$

- Residual for channel *j* at data point *i*

$$f_{j,i}(x) = S_{\text{exp}} - S_{\text{sim}}$$

- w_j is weight applied to each channel

Fitted Experimental Data, Channel 11

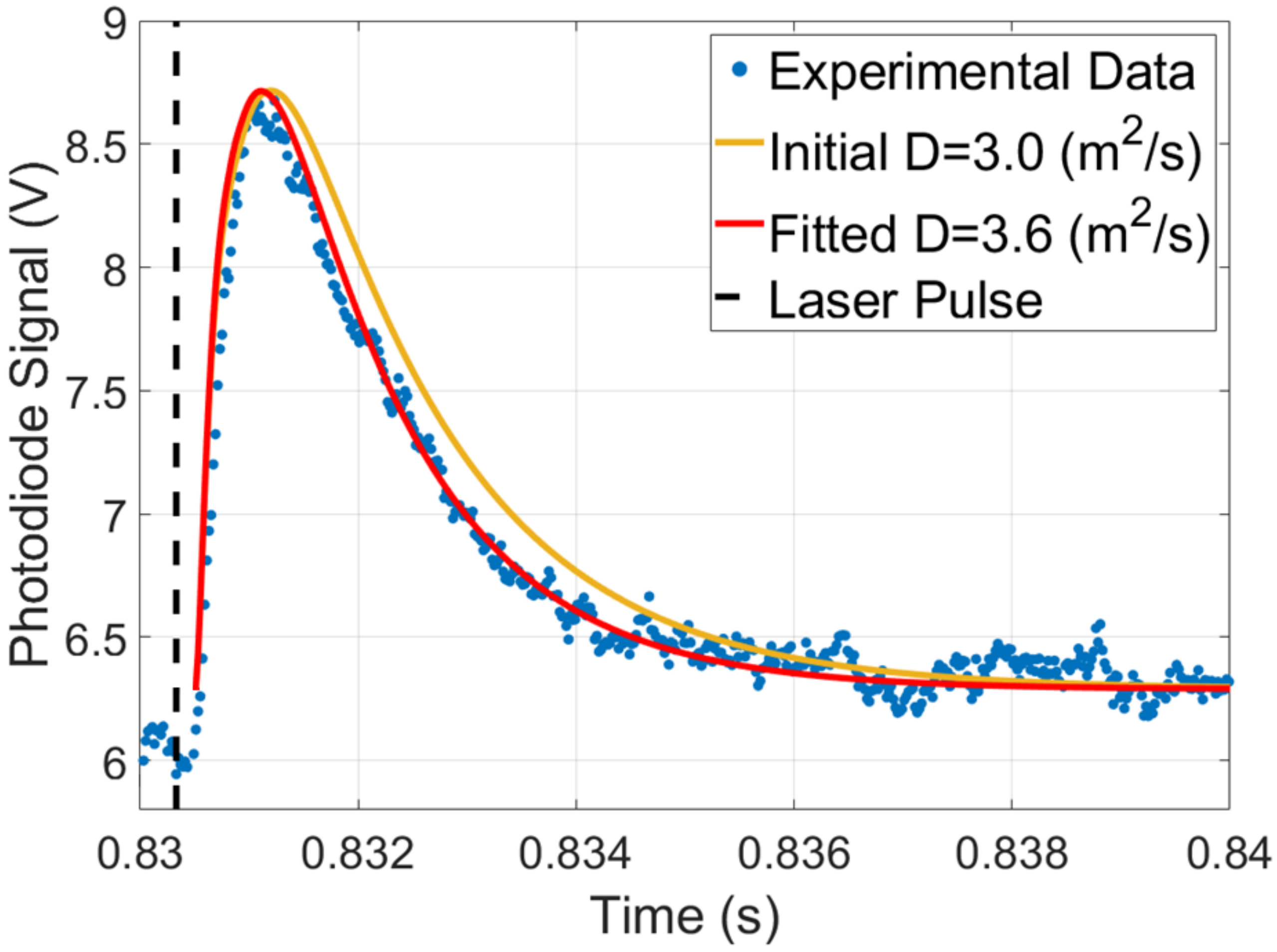

Off-Axis heating varies absorbed power

Many impurity transport experiments determine how impurity confinement time varies with power

- Varying the location where power is deposited in plasma changes the absorbed power
- Absorbed power decreases as heating location is moved away from on-axis core heating
- Electron line-average density kept constant at 3×10^{18} m^{-3} in order to determine reproducibility
- 6 discharges for each heating locations – $r/a \approx 0$ (on-axis), $r/a \approx 0.2,\ r/a \approx 0.3,\ r/a \approx 0.4$

Comparing T_e Profiles

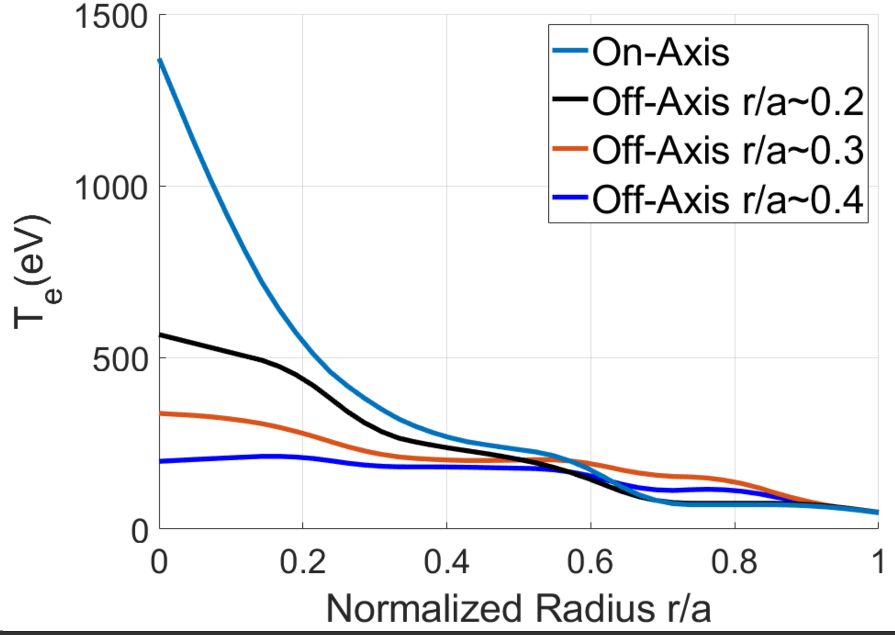

Comparing Signals from 2 Heating Locations

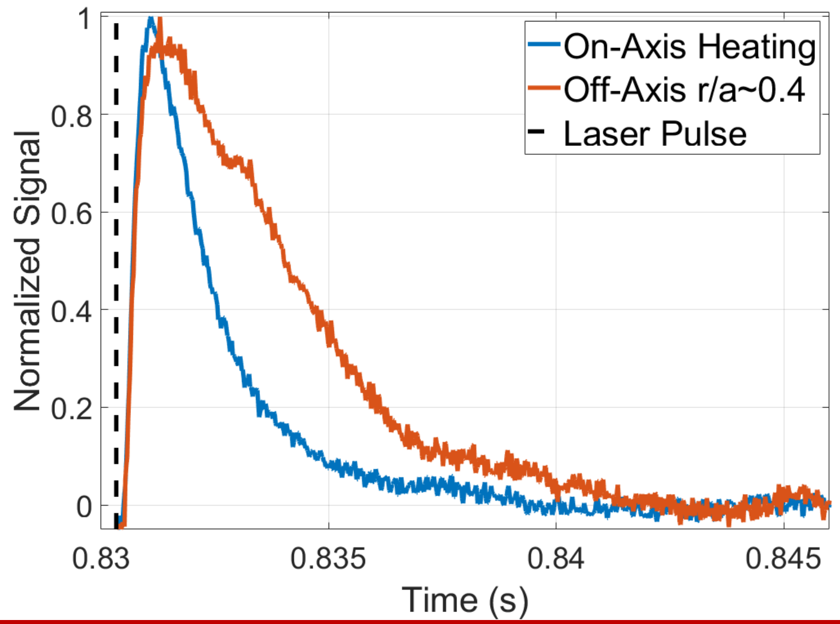

Diffusivity is 2 orders of magnitude more than neoclassical predictions

Experimentally-Inferred Diffusivity

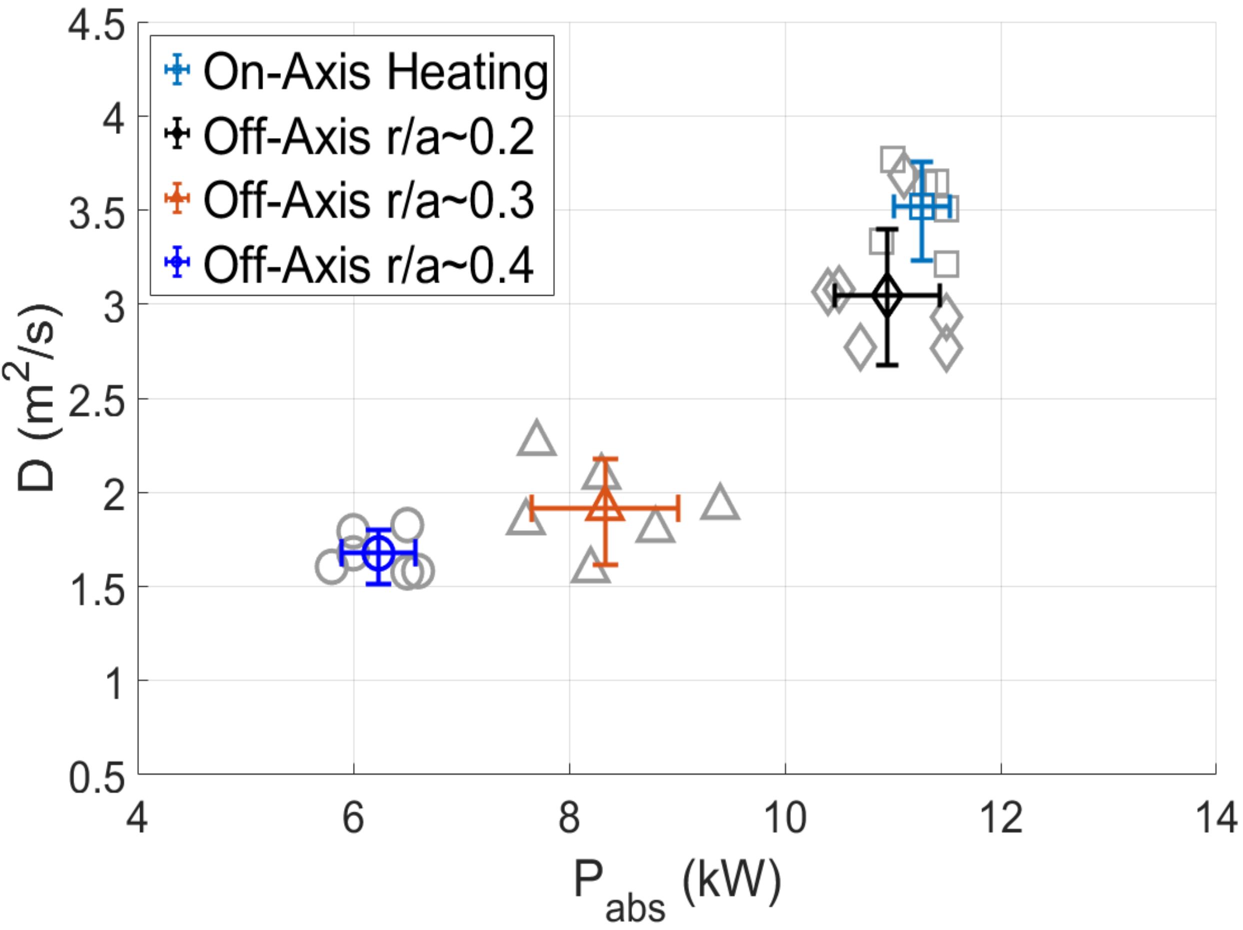

Neoclassically-Predicted Diffusivity

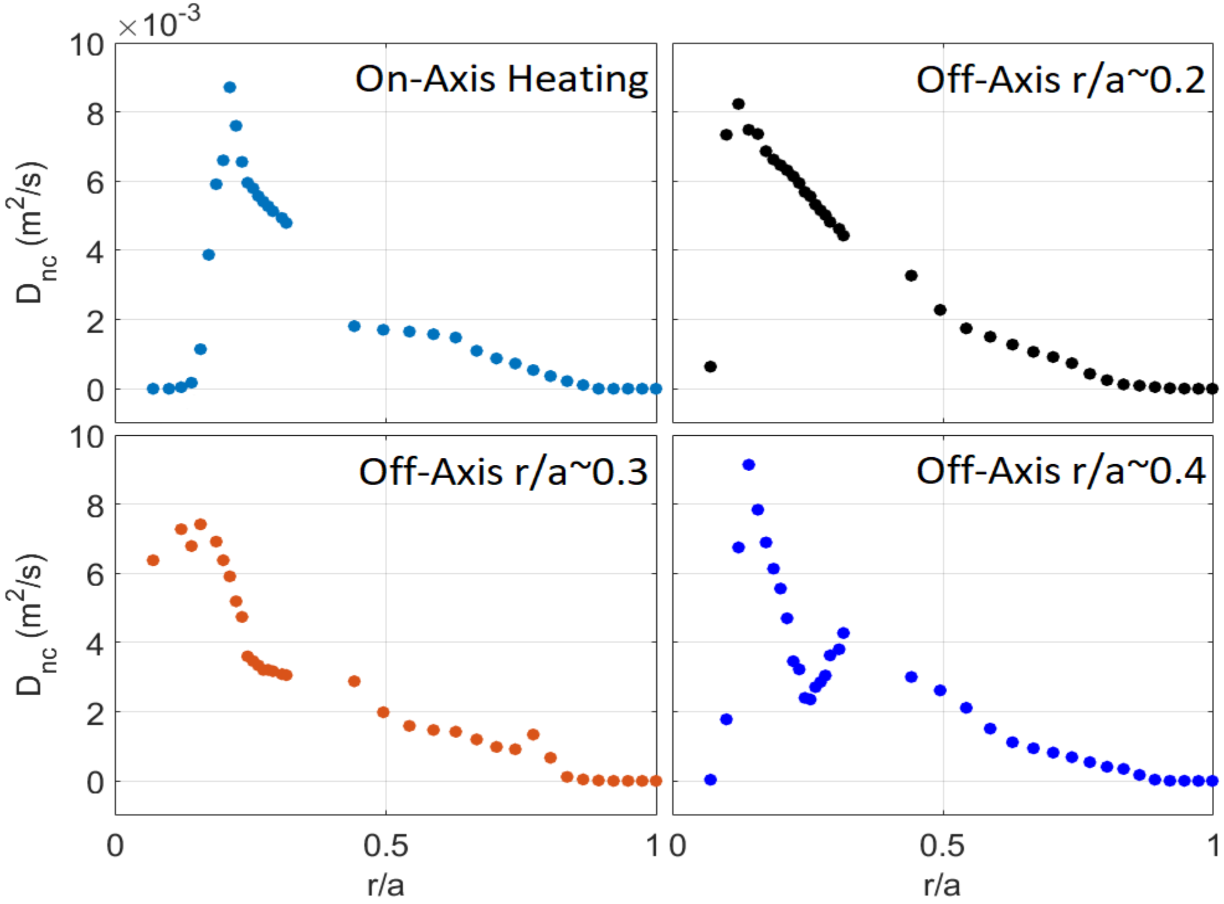

Neoclassical diffusion alone is insufficient to explain these results

Uncertainty studies show inferred diffusivity is well-constrained

Uncertainty Analysis – investigate how STRAHL input variables affect inferred diffusivity

- Electron temperature T_e and density n_e profiles
- Neutral hydrogen density n_H profile
- Scrape-off layer loss time τ_{sol}
- σ_D = Standard deviation of *D* values for 6 discharges

Total Propagation of Uncertainty

$$\delta_{tot} = \sqrt{{\delta_{T_e}}^2 + {\delta_{n_e}}^2 + {\delta_{n_H}}^2 + {\delta_{\tau_{sol}}}^2 + {\sigma_D}^2}$$

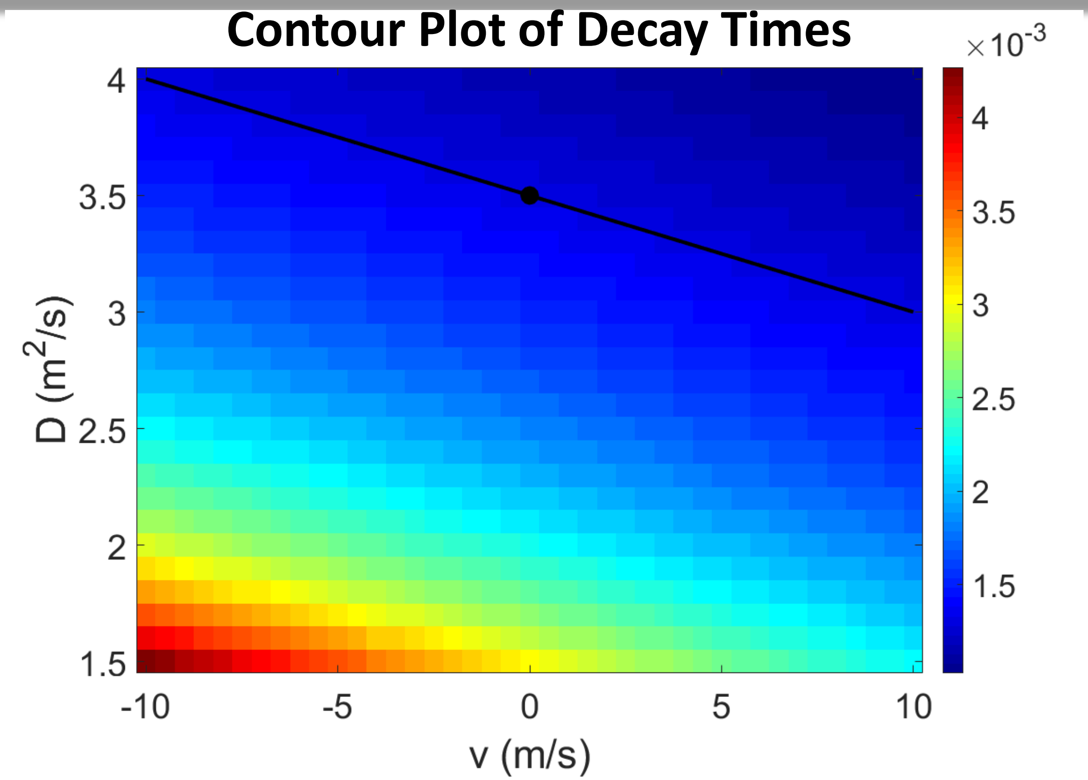

Sensitivity Study – Impurity convective velocity component v

- Plot shows calculated decay times of each D and v combination
- $-10 < v_{nc} < +10$ is 1 order of magnitude smaller and larger than neoclassical PENTA predictions
- D must be constrained between 3-4 m^2/s for 'typical' parameters

STRAHL modeling shows impurity confinement time can be measured after 1 ms

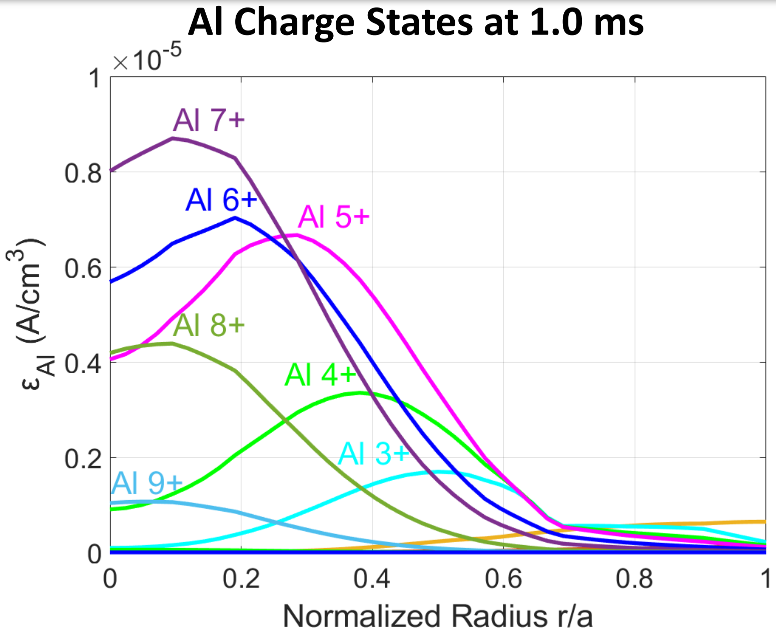

Al charge state emissivities

- 1.0 ms after LBO discharge
- Dominant charge states occur at core region
- Higher charge states

Al 7+, Al 8+, Al 9+

LOS integrated charge states of emissivity

- Black line is total sum of all LOS integrated signals
- After 1 ms (red), slope of total emissivity is the same as highest charge states

A common technique to deduce impurity confinement time is by measuring decay time of the highest observable charge state

Diode measurement single discharge

- Dashed line represents LBO laser pulse
- Data is fitted to exponential curve $e^{-t/\tau_{exp}}$ after 1 ms has elapsed

Average decay time for 6 discharges is:

$$\tau_{exp} \approx 1.52 \pm 0.11 \text{ ms}$$

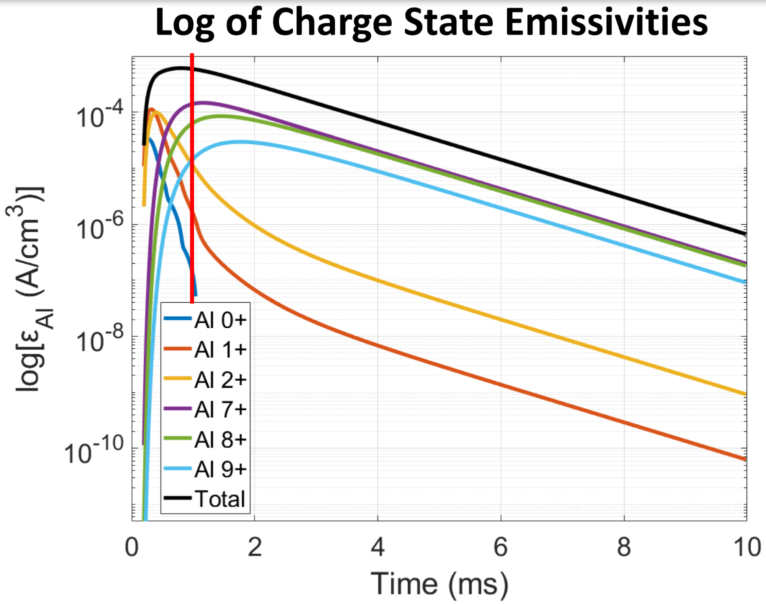

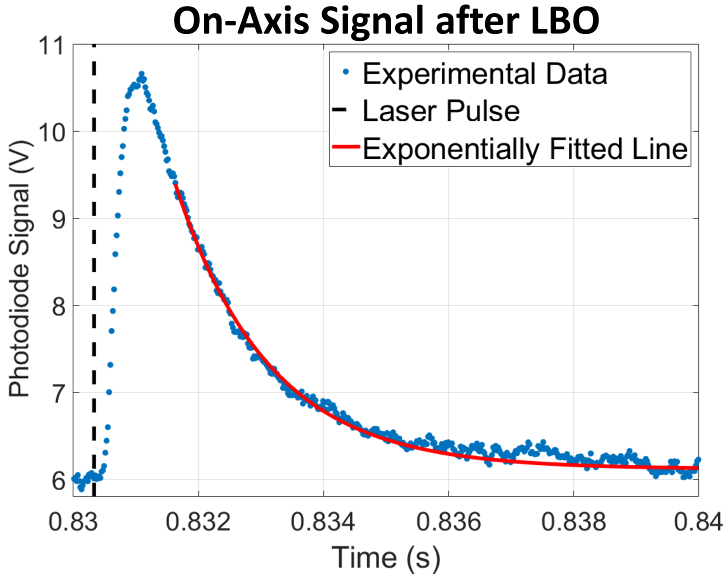

Dependence of impurity confinement on power exhibit a τ~P^{-1} scaling

Impurity transport experiments commonly determine how confinement time scales with power

- Power scaling dependence where $\alpha = 1.0$

$$\tau_{imp} \sim P_{abs}^{-\alpha}$$

- ISS04 unified scaling law approximates $\alpha = 0.61$ for energy confinement

  Yamada, H. et al., Nucl. Fusion. 45 00295515 (2005).

- Nearly all ISS04 discharges are dominated by anomalous transport

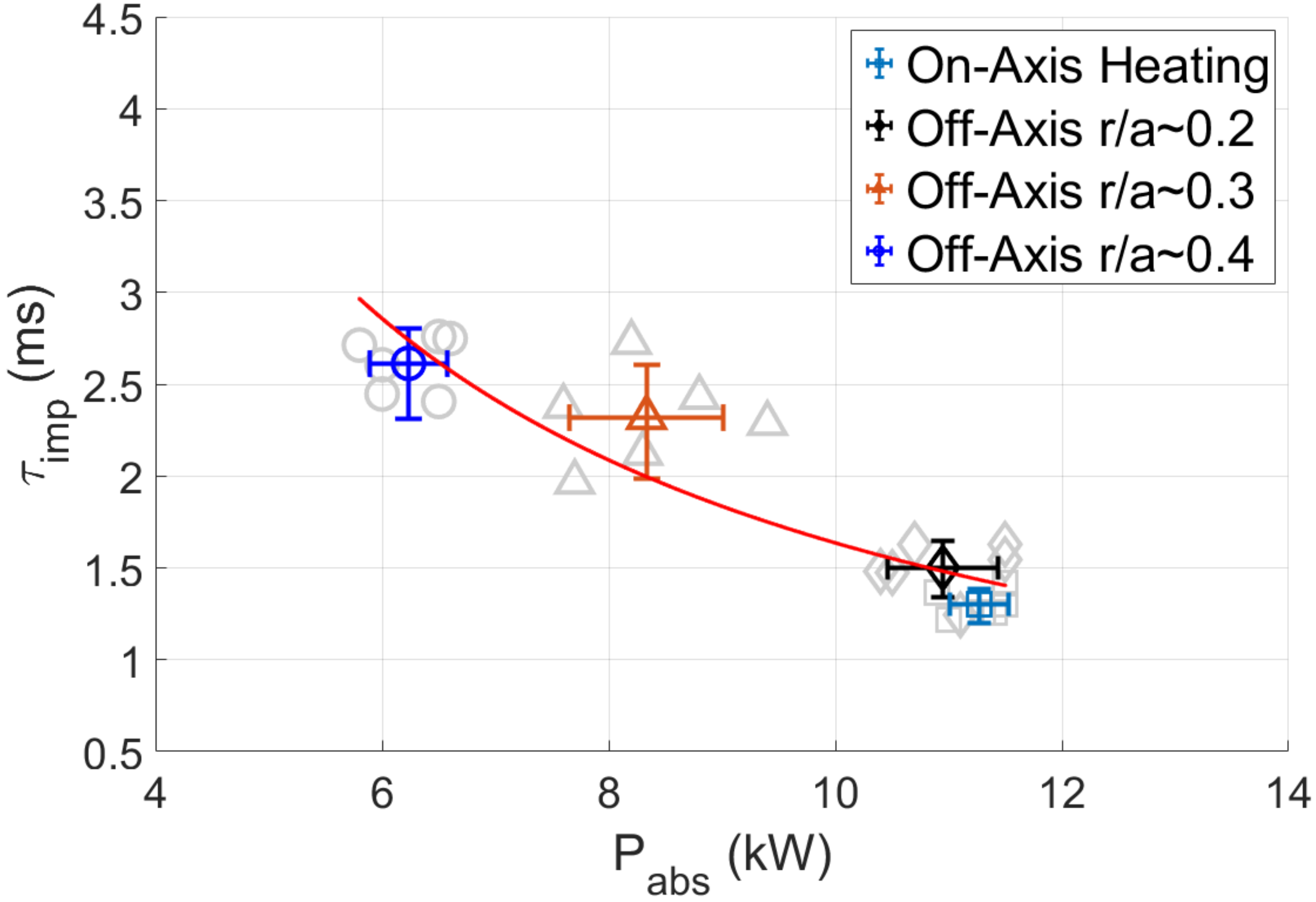

This suggests a substantial impact of turbulence on the impurity transport.

Summary

Key Results

- The LBO system provided good signal-to-noise ratio without strong density perturbation.
- Signals measured were reproducible with similar decay results for each set of experiments.
- The synthetic diagnostic obtained simulated signals that closely match experimental core signals.
- Analysis of modeled STRAHL emissivity shows that at HSX parameters, impurity confinement time can effectively measured 1 ms after laser pulse.
- The impurity diffusivity, being 2 orders of magnitude more than neoclassically-predicted values, is experimental proof the neoclassical diffusion alone is insufficient to explain these results.
- Studies of the dependence of the impurity confinement on the absorbed ECH power exhibit a $\tau \sim \mathrm{P}^{-1}$ scaling, similar to the ISS04 scaling, suggesting a substantial impact of turbulence on the impurity confinement in HSX.

Acknowledgements

Special thanks to David T. Anderson, Aaron Bader, Benedikt Geiger, Santhosh Kumar, Konstantin Likin, Christopher Clark and the whole HSX Lab team.

This work is supported by US DOE Grant DE-FG02-93ER5422.